MJFAS
Malaysian Journal of Fundamental and Applied Sciences

Iqbal *et al.* | Malaysian Journal of Fundamental and Applied Sciences, Vol. 20 (2024) 514-527

RESEARCH ARTICLE

Exploration of Ca^{+2} Binding Affinity to DEAD-Box Helicase through Computational Approaches

Shehryar Iqbal[a]*, Zafar Iqbal[b]*, Hamid Hussain[b], Usman Mauvia[c], Muhammad Sajid Rehman[d], Ali Raza[b]

[a]Department of National Center of Bioinformatics, Quaid-i-Azam University, 44000 Islamabad, Pakistan; [b]Department of Computer Science, MY University, Islamabad, 44000, Pakistan; [c]Department of Computer Science, Comsats University, Islamabad, 44000, Pakistan; [d]Department of Computer Science, Qurtuba University of Sci. & IT, Peshawar, 25000, Pakistan

Abstract Catecholaminergic polymorphic ventricular tachycardia (CPVT) is an occasional catastrophic fatal autosomal dominant or recessive inherited disease that affects an estimated ≈1-5000/10000 people including children, adolescents and young adults, which may cause syncope, abrupt cardiac death during exercise and emotional state. Calmodulin (CALM) functions as a messenger protein of intracellular Ca^{+2} signaling in cardiomyocytes that transmits complex Ca^{+2} ions to the proteins involved in cardiac contraction, and its activation is also facilitated by the binding of Ca^{+2} ions. CALM structure contains 4 EF-hands, each EF-hand holds a single Ca^{+2} ion (designated as, CA149, CA150, CA151 and CA152). In this study, we performed detailed *in_silico* analysis of normal and mutated (ASN53ILE) CALM structures to characterize their Ca^{+2} binding abilities. In $CALM^{-ASN53ILE}$-Pep-IQ complex, we observed a binding shift of P68(Pep-IQ) as compared to $CALM^{-WT}$. The root mean square deviation was in the range of 0.4-1 nm for all the systems, while root mean square fluctuation values were in the range of 0.3-0.6 nm for bound versus unbound proteins. Hydrogen-bond profiling was significantly different between $CALM^{-WT}$ and $CALM^{-ASN53ILE}$ over the course of simulation. We observed an introduction of β1 and β2-segment between α1- α2 and α3- α4 along with the movement of C-terminal approximately to 180^0 in the apo-$CALM^{-ASN53ILE}$. Thus, we propose that, ASN53ILE has a pathological impact in the progression of CPVT due to structural and conformational changes in CALM and its binding affinity towards P68(Pep-IQ). The current study may constitute a valuable starting point for CPVT therapeutics through the involvement of $CALM^{-ASN53ILE}$ for designing novel inhibitors to cope with neuropathological disorder.

Keywords: CPVT, Calmodulin (CALM), in_silico analysis, P68(Pep-IQ), pathological impact, conformational changes, Neuropathological disorder.

***For correspondence:**
zafar.iqbal@myu.edu.pk

Received: 14 Dec. 2023
Accepted: 14 April 2024

Introduction

Catecholaminergic polymorphic ventricular tachycardia (CPVT), commonly known as catastrophic mortal, is a genetic disease (sporadic cardiac ion channelopathy), that is characterized by incomprehensible sudden cardiac death (SCD) observed in children [1]. When left untreated, the disease's extinction rate increases significantly, reaching 31% by the age of 30 year [2]. The study evaluated the occurrence of cardiac rates over a period of 4 to 8 years, ranging from 33% to 58% in patients' progression [3]**.** The disease is caused by the calmodulin (CALM) structural changes, which usually contain a hereditary background for CPVT [4, 5]. It has been reported that novel structural changes in CALM are linked with this disorder [6]. CALM acts as a crucial player in regulating several ion channels in the heart [7]. The disease (CPVT) has been associated to CALM mutations, which code for the heart sarcoplasmic Ca^{+2} channel. The association of CPVT-related variant (c.161A>T; CALM-

^{ASN53ILE}) with large Swedish family was found having serious dominantly inherited character of CPVT-like arrhythmias. A genome-wide association studies (GWAS), revealed that CALM1$^{-ASN53ILE}$ has the heterozygous missense genetic inheritance pattern in CPVT [8]. It has been reported that serious cardiac arrhythmia can be produced due to CALM mutations and CALM should be tested for idiopathic ventricular tachycardia [9].

RNA helicase p68, a potential ATP-dependent RNA helicase, is recognized as the original RNA helicase from the DEAD-box family (DDX5) [10]. The DDX5 group comprises of 38 member proteins that are involved in every stage, which is required for cells to properly function in many ways, such as proliferation, embryogenesis, RNA ribosome biogenesis, and cell growth [11]. Several RNA helicases including p68 have been discovered, which perform a significant role in the tumor growth having the potential to control gene expression and explain the aberrant expression in diverse malignancies. It is usually up-regulated in numerous malignant and performs as a transcriptional co-activator for several transcription factors, with CALM Ca^{+2} receptor [10]. The previous study reveals that p68 interacts with cancer metastasis and cell migration, by interacting with CALM. In two different animal models, a peptide fragment that crosses the p68-IQ motif outstandingly reduces cancer metastasis. The peptide prevents the interaction of both p68 and CALM, which suppresses cell migration. It is demonstrated that the interaction of p68-CALM interaction is significant for the development of lamellipodia and filopodia in migrating cells. P68 attracts microtubules when CALM is available. It has been found that p68 ATPase activity is stimulated by contact with microtubules. Furthermore, microtubule gliding studies demonstrate that p68 can perform as a microtubule motor when CALM is present. CALM may be delivered by p68 to the leading edge of migrating cells when permitted by this motor activity [12].

In this study we performed the exploration of a therapeutic strategy for (CPVT) by comparative interaction pattern of human protein CALM^{-WT} and CALM$^{-ASN53ILE}$ with Pep-IQ of RNA helicase p68 (DDX5) protein. CALM functions as a messenger protein of intracellular Ca^{+2} signaling in cardiomyocytes which transmits complex Ca^{+2} transient to the proteins regulating cardiac contraction, and its activation is also facilitated by the binding of Ca^{+2} ions. CALM structure contains 4 EF-hands, each EF-hand holds a single Ca^{+2} ions. The impact of Ca^{2+} ions in CALM^{-WT} and CALM$^{-ASN53ILE}$ with P68-PepIQ may assist in conformational and structural readjustments during pathological progression of disease at the molecular and atomic level.

Materials and Methods

Dataset

3D structure of CALM (PDBID: 4DJC) having 4 Ca2+ ions and primary protein sequence of p68 (Pep-IQ) (UniProt ID: P17844; 2.7 Å) was retrieved through UniProtKB/Swiss-Prot database. The suitable templates were isolated using NCBI Protein-Protein BLAST against Protein data bank (PDB) database [13]. The homology modeling method was performed to predict the structure of Pep-IQ (VSAGIQTSFRTGNPTG) of p68. MODELLER 9.17 was used for homology or comparative modeling of protein 3D structures [14]. Visualization and Superimposition of 3D protein structures was performed using UCSF Chimera [15]. The prognosticated and modeled P68 (DDX5) structures were improved through 1000 steps of steepest-decent [16] and 1000 steps of conjugate-gradient[17], minimization by UCSF Chimera version 1.15 [18], through GROMOS9643a1 extended phosphorylated force field. Eventually, Wincoot was utilized to repair Ramachandran outliers and bad rotamers to achieve the hone and true structure for additional computational research. The stereo chemical properties and Ramachandran values were evaluated by Molprobity Server [19].the detailed work methodology presented in Figure 1.

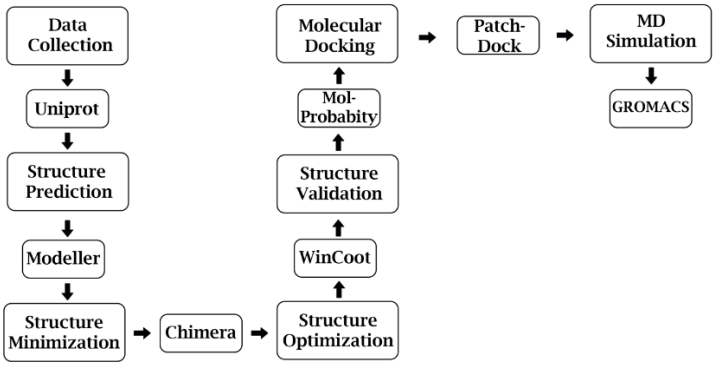

Figure 1. Flow chart of the work methodology

Molecular Docking Analysis

Molecular docking analysis of CALM and P68 (Pep-IQ) was accomplished through PatchDock and the fixed refinement tool FireDock. PatchDock is a web-based server that performs geometry-based molecular docking analysis through a segmentation algorithm by surface matching and filtering based on the truncated energy pose, a scoring function that appraises geometric fit and atomic desolvation energy [20] to calculate each applicant transformation. Finally, the most relevant applicant solution was selected among the dispensable solutions based on RMSD (Root Mean Square Deviation) clustering.
To revalidate that binding of CALM and P68 (Pep-IQ), molecular docking analysis was executed through ClusPro [21]. ClusPro is an automated online server for protein-protein docking that utilizes the Fourier correlation algorithm for the fast refinement of results by using a combination of desolvation and electrostatic energies. Closely inherent structures are allowed through the filter, resulting in the deletion of incorrect positive output. Cluspro was used to perform docking analysis to notice the protein-protein interaction [22]. Cluspro uses the pairwise potential of a stiff body docking program (PIPER) that is based on the Fast Fourier Transform (FFT) technique for docking; however, about a thousand appropriate energy values are clustered, from which 30 large clustered are chosen for the cleansing with the help of detection of native and non-native clusters. Monto Carlo simulation is utilized for stabilizing the clusters while refinement is performed by Semi-Definite programming-based Underestimation (SDU). Models were ranked according to the lowest docking energy values and cluster sizes. We observed saturated clusters of best models in all categories. The binding interaction was thoroughly examined through UCSF Chimera 1.15 [18].

Molecular Dynamics Simulation Assays

Molecular dynamics (MD) is a simulation approach used to study the behavior of macromolecules and the time evolution of interacting particles. It is based on Newton's laws of motion, quantum mechanics, and classical mechanics laws. To acquire additional intuition CALM and P68 (Pep-IQ) interaction, MD simulation assays were performed through GROMACS 5.1.4 [23]. GROMOS9643a1 extended phosphorylated force field with spc216 water model was utilized to simulate the protein complex accompanied by the computation of suitable electrostatic counter ions to nullify the system. Before the MD simulation run, energy minimization was carried out by the steepest-decent method (5000 steps) [16] with a forbearance of 1000 kJ/mol/nm to eliminate the initial steric clashes. The system's stability was attained under the control of periodic boundary circumstances utilizing an octahedran box 12 × 12 × 11 nm. Conclusively, an MD simulation run was performed for 150 ns under the control of constant temperature (300 K) and Pressure (1 ATM) in NVT [24] and NPT [24] accumulates, respectively. Trajectory analysis was studied by determining RMSD (Root Mean Square Deviation) and RMSF (Root Mean Square Fluctuations) to examine the system's reliability and functioning. For observing the conformational changes, PDB files were generated at different time scales and then analyzed by UCSF Chimera. The stability and functioning of each single system were studied through VMD and GROMACS tools [23].

Results and Discussion

Structure Retrieval of CALM

The structure of CALM was retrieved through RCSB PDB (PDB ID: 4DJC). It possesses 4 Ca^{+2} ions in each EF-hand. The EF hand is a structural motif or domain that possesses helix-loop-helix conformation in Ca^{+2}-binding proteins. Based on the observation that CALM is a Ca^{+2} modulating protein, the presence or absence of Ca^{+2} may affect the binding with other interacting proteins. In order to understand the influence of Ca^{+2} ions, each Ca^{+2} ion was deleted individually Figure 2 and the modified structure was validated using MolProbity Server.

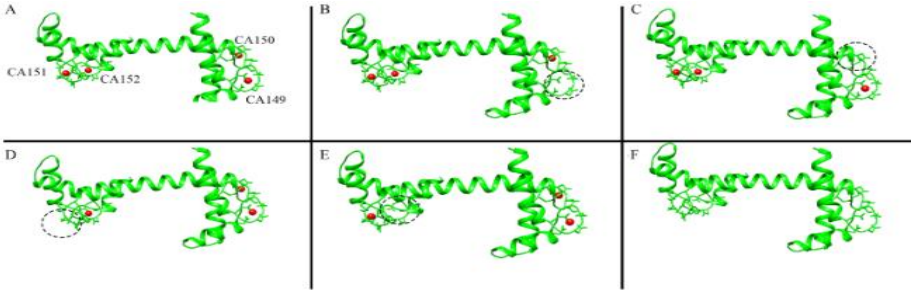

Figure 2. Crystal structure of CALM**.** A. CALM possessing all Ca^{+2} ions (red sphere), B. Deletion of Ca^{+2} ion from 1st EF-hand (-CA149) highlighted in a dotted circle, C. Deletion of Ca^{+2} ion from 2nd EF-hand (-CA150) highlighted in a dotted circle, D. Deletion of Ca^{+2} ion from 3rd EF-hand (-CA151) highlighted in a dotted circle. E. Deletion of Ca^{+2} ion from 4th EF-hand (-CA152) highlighted in a dotted circle and F. All Ca^{+2} deleted from EF-hands

Molecular Modeling of P68 (Pep-IQ)

In order to get the complete 3D structure of p68, multiscale structure-based studies were carried out. The template was chosen on the basis of high sequence identity (81.82%) and query coverage values (62%) having an E-value of 0.37. Ramachandran plot designated the presence of more than 100% residues of P68(Pep-IQ) structure in the sterically allowed region with no poor rotamers Figure 3. The parameters like peptide bond planarity, non-bonded interactions, C α-tetrahedral distortion, main chain H-bond energy, and the overall G-factor for the modeled structure were lying in the favorable range.

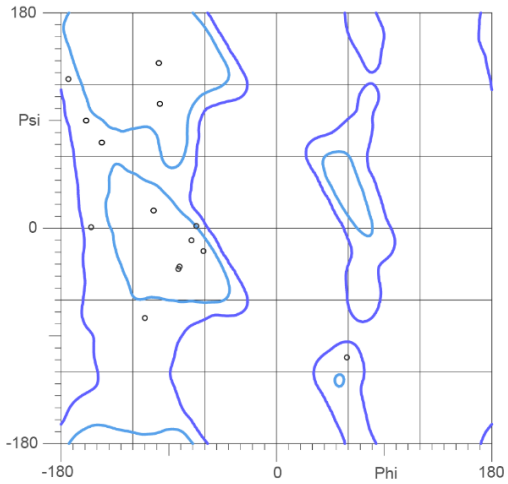

Figure 3. Ramachandran plot P68-Pep-IQ. Structural validation of P68 (Pep-IQ). Small circles (Black) indicate each amino acid in sterically allowed regions

Molecular Docking and Interaction Analysis of CALM and P68

Molecular docking analysis was performed using the PatchDock server in order to find the interactive residues of CALM and P68(Pep-IQ) that revealed their substantial binding poses. Docking was conducted with default parameters in which clustering RMSD was 4.0. Investigation of the binding contribution of conserved residues was carefully carried out indicating similar conserved regions of both proteins. Elimination of Ca^{+2} ion may affect the binding of CALM with Pep-IQ of p68; not all Ca^{+2} ions equally contribute in the binding. On the basis of binding analysis, these 8 complexes were divided into 2 groups that possessed different binding patterns Figure 4. Pep-IQ of p68 complexes with normal $CALM^{-WT}$, $CALM^{-WT,\ del\ CA149}$, $CALM^{-WT,\ del\ CA150}$, $CALM^{-WT,\ del\ CA151}$, $CALM^{-WT,\ del\ CA152}$ possessing similar interaction patterns were designated as group-I, while other mutant complexes ($CALM^{-\ ASN53ILE,\ del\ CA149}$, $CALM^{-\ ASN53ILE,\ del\ CA150}$, $CALM^{-\ ASN53ILE,\ del\ CA151}$, $CALM^{-\ ASN53ILE,\ del\ CA152}$) were categorized in group-II.

The PatchDock specific predicted energy values of Group-I complexes $CALM^{-WT}$, $CALM^{-WT,\ del\ CA149}$, $CALM^{-WT,\ del\ CA150}$, $CALM^{-WT,\ del\ CA151}$, $CALM^{-WT,\ del\ CA152}$ in association with P68(Pep-IQ) peptides were -822.6 kcal/mol and -781.6 kcal/mol, -642.6 kcal/mol and -497.6 kcal/mol and -424.6 kcal/mol Table 1, respectively. While, predicted energy values of Group-II complexes $CALM^{-ASN53ILE}$, $CALM^{-ASN53ILE,\ del\ CA149}$, $CALM^{-ASN53ILE,\ del\ CA150}$, $CALM^{-ASN53ILE,\ del\ CA151}$, $CALM^{-ASN53ILE,\ del\ CA152}$ in association with P68(Pep-IQ) were -751.7 kcal/mol -621.7 kcal/mol, -615.7 kcal/mol, -479.7 kcal/mol and -296.7 kcal/mol Table 2, respectively.

Table 1. Group-I complexes with their binding energies

No.	CALM-P68(Pep-IQ)	Binding Energy (kcal/mol)
1	$CALM^{-WT}$ –P68(Pep-IQ)	-822.6
2	$CALM^{-WT,\ del\ CA149}$ –P68(Pep-IQ)	-781.6
3	$CALM^{-WT,\ del\ CA150}$ –P68(Pep-IQ)	-642.6
4	$CALM^{-WT,\ del\ CA151}$ –P68(Pep-IQ)	-497.6
5	$CALM^{-WT,\ del\ CA152}$ –P68(Pep-IQ)	-424.6

Table 2. Group-II complexes with their binding energies

No.	CALM-P68(Pep-IQ)	Lowest Binding Energy (kcal/mol)
1	CALM$^{-ASN53ILE}$-P68(Pep-IQ)	-751.7
2	CALM$^{-ASN53ILE, del CA149}$ –P68(Pep-IQ)	-621.7
3	CALM$^{-ASN53ILE, del CA150}$ –P68(Pep-IQ)	-615.7
4	CALM$^{-ASN53ILE, del CA151}$ –P68(Pep-IQ)	-479.7
5	CALM$^{-ASN53ILE, del CA152}$ -Pep-IQ	-296.7

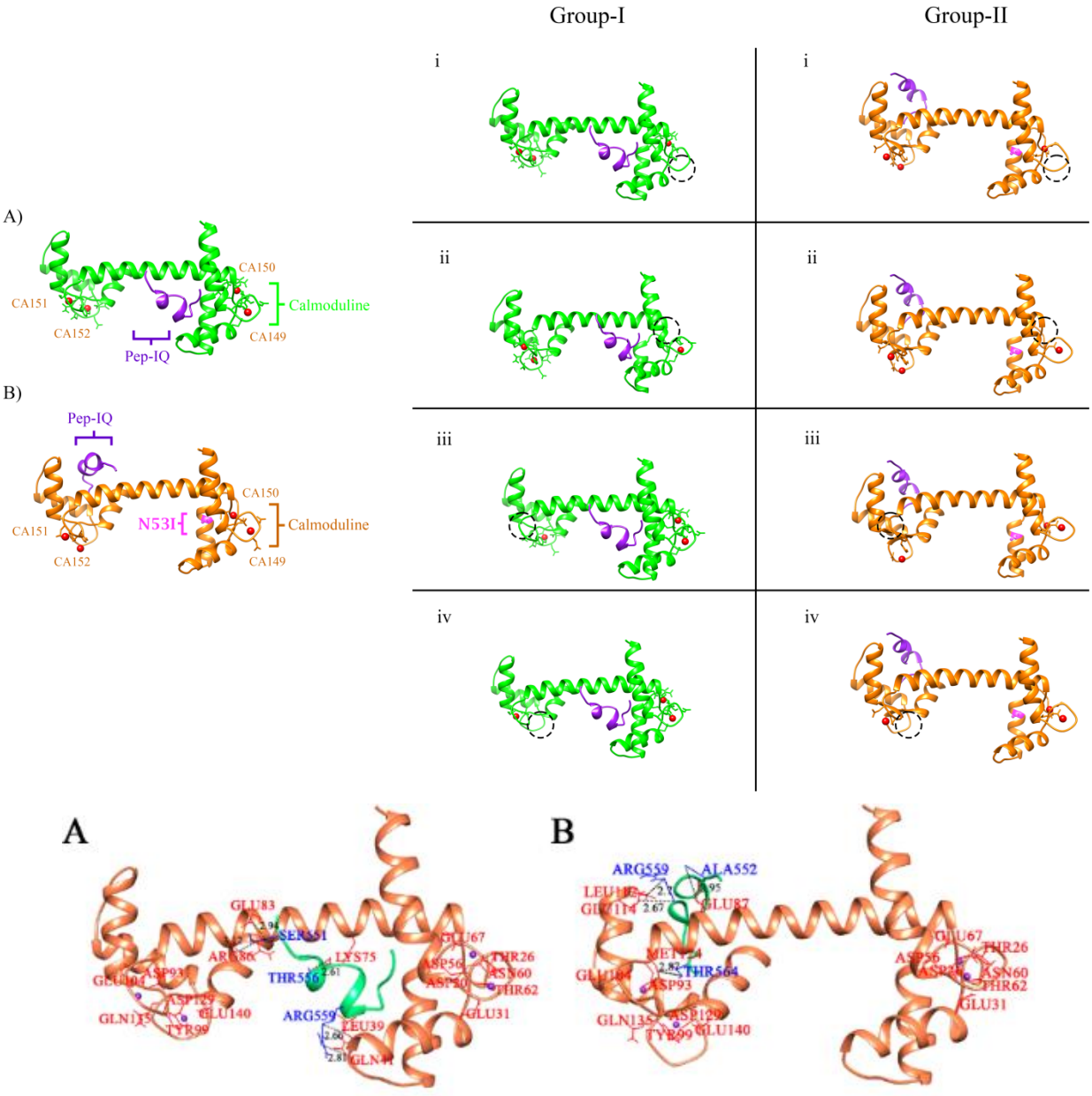

Figure 4. Molecular docking analysis of CALM and P68(Pep-IQ). **A)** CALM^{-WT}-P68 (Pep-IQ) possessing all Ca^{+2} ions **i.** -CA149 **ii.** -CA150 **iii.** -CA151 **iv.** -CA149 highlighted in a dotted circle, **B)** CALM$^{-ASN53ILE}$-P68(Pep-IQ) possessing all Ca^{+2} **i.** -CA149 **ii.** -CA150 **iii.** -CA151 **iv.** -CA149 highlighted in a dotted circle. CALM^{-WT} (A) and its respective group-I are shown and labeled in green color, while CALM$^{-ASN53ILE}$ (B) and its respective group-II are shown and labeled in orange color. Pep-IQ is shown and labeled in purple color. Ca^{+2} ions are shown and labeled in red color. Mutation in CALM$^{-ASN53ILE}$ is shown in pink color respectively

Binding Analysis of Group-I (CALM^{-WT}-P68(Pep-IQ)) in Comparison with Group-II (CALM$^{-ASN53ILE}$-P68 (Pep-IQ))

To analyze the interaction of group-I and group-II complexes with P68(Pep-IQ), molecular docking analysis was performed individually Figure 4. The ideal complexes were selected on the basis of least energy value interaction pattern. The group-I and group-II complexes were visualized individually through LigPlot. Evidently, LEU39, GLN41, LYS75, GLU83 and ARG86 residues of CALM^{-WT}, CALM$^{-WT, del CA149}$, CALM$^{-WT, del CA150}$, CALM$^{-WT, del CA151,}$ CALM$^{-WT, del CA152}$ exhibited interactions with SER551 THR556 and ARG559 residues of Pep-IQ of p68, while group-II complexes evidently, ASN108, GLU111, GLU124 and MET141 residues of CALM$^{-ASN53ILE}$, CALM$^{-ASN53ILE, del CA149}$, CALM$^{-ASN53ILE, del CA150}$, CALM$^{-ASN53ILE, del CA151}$, CALM$^{-ASN53ILE, del CA152}$ exhibited interactions with VAL550, GLN555, THR564 and ASN562 residues of Pep-IQ of p68 respectively Figures 5-9. With exception of CALM$^{-ASN53ILE}$ specific residues GLU84, LEU109 and MET121 were in interaction with P68(Pep-IQ) specific residues GLY553, ARG559 and THR56. Residual same interaction patterns illustrate within group-I but different interaction patterns between group-I and group-II were also visualized through PDBSum Figure 10. Apart from hydrogen-bonded residues, multiple hydrophobic contacts were also involved Table 3 & 4.

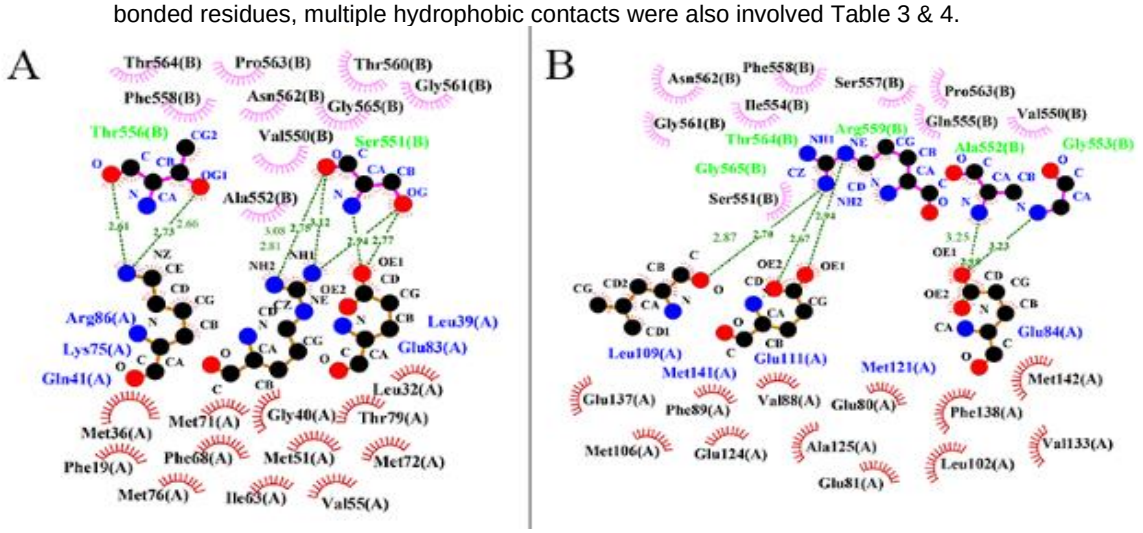

Figure 5. LigPlot interaction analysis of group-I and group-II with P68(Pep-IQ). Schematic diagram representing the interactions of group-I (CALM^{-WT}) and group-II (CALM$^{-ASN53ILE}$) protein with Pep-IQ of p68. CALM$^{-WT,}$ residues (labeled in blue) exhibit hydrogen bonding with P68(Pep-IQ) residues (labeled in green). CALM$^{-ASN53ILE}$ residues (labeled in blue) exhibit hydrogen bonding with P68(Pep-IQ) residues (labeled in orange). Residues exhibiting hydrophobic interactions are labeled in black. The amino acids involved in hydrophobic interactions are shown in magenta (Pep-IQ) and red (CALM) are labeled in black in both complexes. The atoms of amino acids involve in hydrogen bonding interactions are labeled in black (CALM) and blue (Pep-IQ) in both complexes

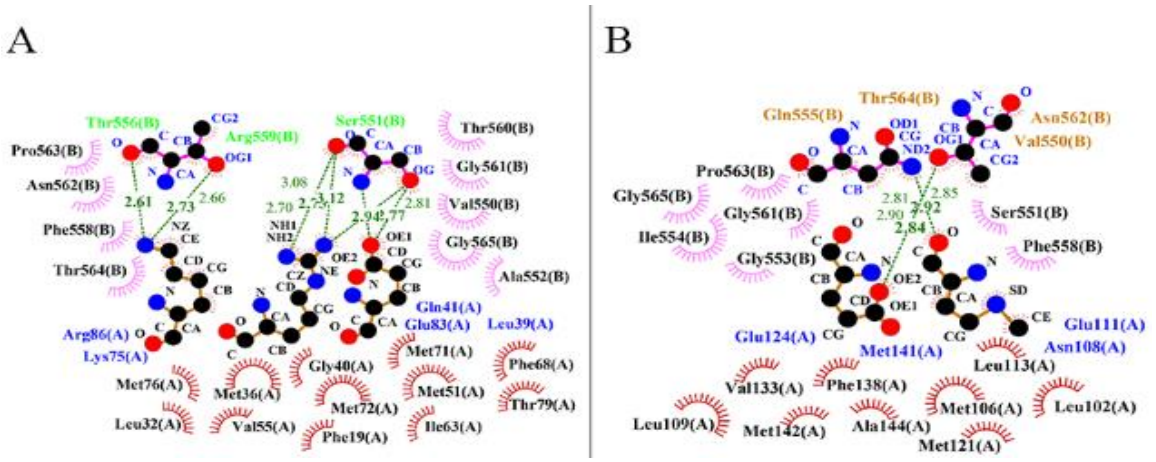

Figure 6. LigPlot interaction analysis of group-I and group-II with P68(Pep-IQ). Schematic diagram representing the interactions of **A**. (CALM$^{-WT, del CA149}$) and **B**. (CALM$^{-ASN53ILE, del CA149}$) with Pep-IQ of p68. CALM$^{-WT, del CA149}$ residues (labeled in blue) exhibit hydrogen bonding with P68(Pep-IQ) residues (labeled in green). CALM$^{-ASN53ILE, del 149CA}$ residues (labeled in blue) exhibit hydrogen bonding with P68(Pep-IQ) residues (labeled in orange). Residues exhibiting hydrophobic interactions are labeled in black. The amino acids involve in hydrophobic interactions are shown in magenta (Pep-IQ) and red (CALM) are labeled in black in both complexes. The atoms of amino acids involved in hydrogen bonding interactions are labeled in black (CALM) and blue (Pep-IQ) in both complexes

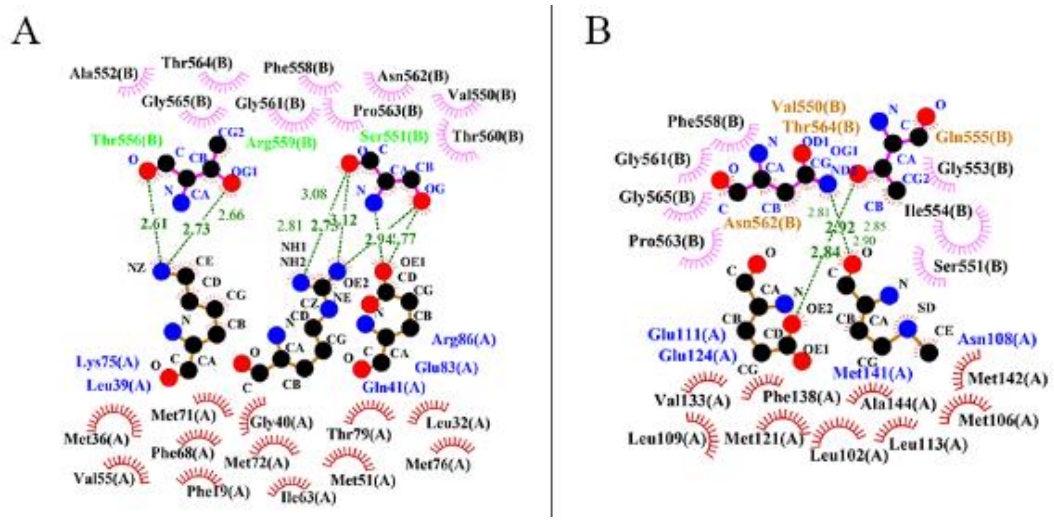

Figure 7. LigPlot interaction analysis of group-I and group-II with P68(Pep-IQ). Schematic diagram representing the interactions of **A.** (CALM$^{-WT,\ del\ CA150}$) and **B.** (CALM$^{-ASN53ILE,\ del\ CA150}$) with Pep-IQ of p68. CALM$^{-WT,\ del\ CA150}$ residues (labeled in blue) exhibit hydrogen bonding with P68(Pep-IQ) residues (labeled in green). CALM$^{-ASN53ILE,\ del\ 150CA}$ residues (labeled in blue) exhibit hydrogen bonding with P68(Pep-IQ) residues (labeled in orange). Residues exhibiting hydrophobic interactions are labeled in black. The amino acids involve in hydrophobic interactions are shown in magenta (Pep-IQ) and red (CALM) are labeled in black in both complexes. The atoms of amino acids involved in hydrogen bonding interactions are labeled in black (CALM) and blue (Pep-IQ) in both complexes

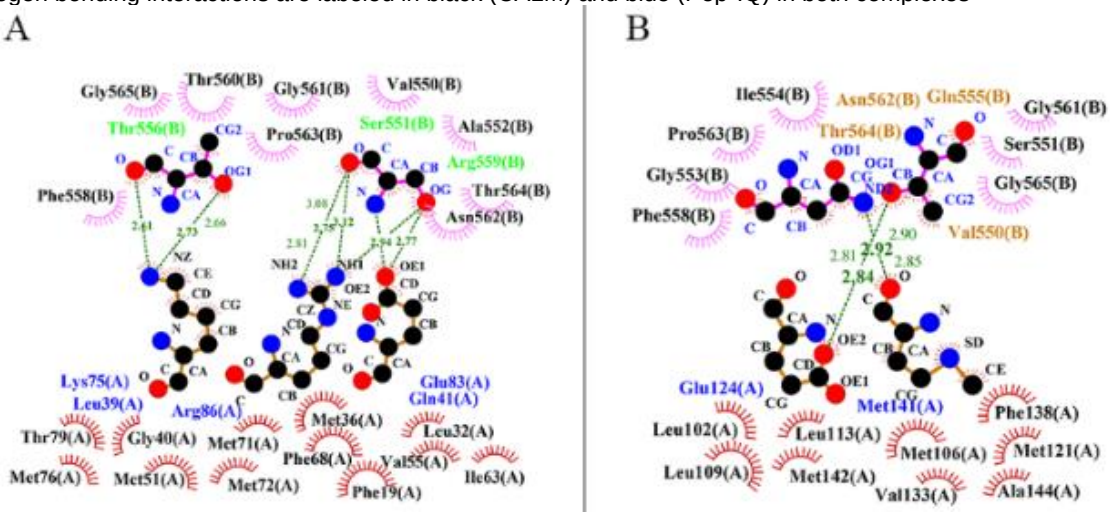

Figure 8. LigPlot interaction analysis of group-I and group-II with P68(Pep-IQ). Schematic diagram representing the interactions of **A**. (CALM$^{-WT,\ del\ CA151}$) and **B**. (CALM$^{-ASN53ILE,\ del\ CA151}$) with Pep-IQ of P68. CALM$^{-WT,\ del\ CA151}$ residues (labeled in blue) exhibit hydrogen bonding with P68(Pep-IQ) residues (labeled in green). CALM$^{-ASN53ILE,\ del\ 151CA}$ residues (labeled in blue) exhibit hydrogen bonding with P68(Pep-IQ) residues (labeled in orange). Residues exhibiting hydrophobic interactions are labeled in black. The amino acids involve in hydrophobic interactions are shown in magenta (Pep-IQ) and red (CALM) are labeled in black in both complexes. The atoms of amino acids involved in hydrogen bonding interactions and are labeled in black (CALM) and blue (Pep-IQ) in both complexes

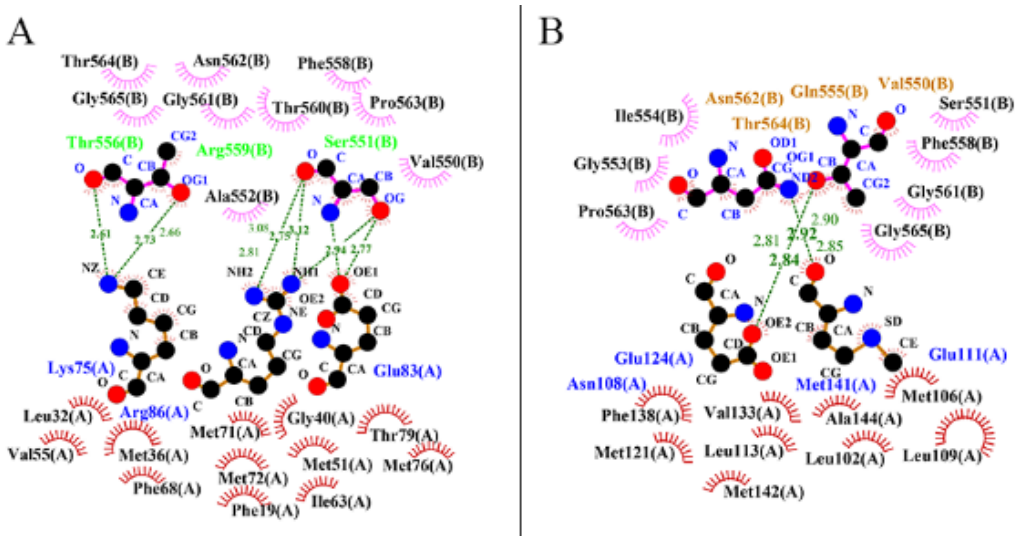

Figure 9. LigPlot interaction analysis of group-I and group-II with P68(Pep-IQ). Schematic diagram representing the interactions of **A.** (CALM$^{-WT,\ del\ CA152}$) and **B.** (CALM$^{-ASN53ILE,\ del\ CA152}$) with Pep-IQ of P68. CALM$^{-WT,\ del\ CA152}$ residues (labeled in blue) exhibit hydrogen bonding with P68(Pep-IQ) residues (labeled in green). CALM$^{-ASN53ILE,\ del\ 152CA}$ residues (labeled in blue) exhibit hydrogen bonding with P68(Pep-IQ) residues (labeled in orange). Residues exhibiting hydrophobic interactions are labeled in black. The amino acids involve in hydrophobic interactions are shown in magenta (Pep-IQ) and red (CALM) are labeled in black in both complexes. The atoms of amino acids involved in hydrogen bonding interactions and are labeled in black (CALM) and blue (Pep-IQ) in both complexes

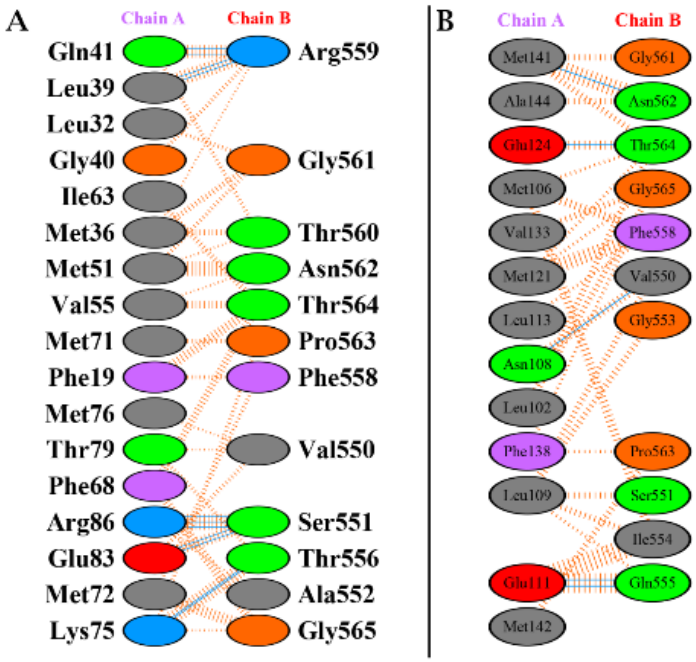

Figure 10. Binding interaction of group-I CALM^{-WT} and group-II CALM$^{-ASN53ILE}$ with P68(Pep-IQ). (A & B) Comparative binding pattern of CALM with Pep-IQ. Positive residues (H,K,R) are indicated in sky blue color, negative residues (D,E) in red color, neutral residues (S,T,N,Q) in green color, aliphatic (A,V,L,I,M) in grey color, while aromatic residues (F,Y,W) in purple color. Hydrogen bonding is indicated with blue line, salt bridges with red lines, while non-bonded contacts with dotted orange lines

Table 3. Molecular docking analysis of Group-I CALM-WT with P68(Pep-IQ)

	Hydrogen bonded residues			Hydrophobic interaction	
Complex	Group-I CALM	P68(Pep-IQ)	H-bond distance (angstrom)	Group-I CALM	P68(Pep-IQ)
Group-I CALM-ASN53ILE -P68(Pep-IQ)	GLU83	SER551	2.77	PHE19	THR564
	ARG86	SER551	2.67	PHE19	PHE558
	LYH75	THR556	2.61	LEU32	GLY561
	LEU39	ARG559	2.66	MET36	GLY561
	GLN41	ARG559	2.70	MET36	ARG559
				MET36	THR560
				LEU39	ARG559
				GLY40	ARG559
				GLN41	ARG559
				GLN41	ARG559
				GLN41	THR560
				MET51	ASN562
				MET51	GLY561
				MET51	THR560
				VAL55	THR564
				VAL55	ASN562
				PHE68	THR564
				PHE68	GLY565
				MET71	PRO563
				MET72	GLY565
				MET72	PHE558
				LYS75	GLY565
				LYS75	THR556
				PHE19	THR564

Table 4. Molecular docking analysis of group-II CALM-AN53ILE with P68(Pep-IQ)

	Hydrogen bonded residues			Hydrophobic interaction	
Complex	**Group-II CALM**	**P68(Pep-IQ)**	**H-bond distance (angstrom)**	**Group-II CALM**	**P68(Pep-IQ)**
Group-II CALM-ASN53ILE -P68(Pep-IQ)	ASN108	VAL550	2.90	LEU102	THR564
	GLU111	GLN555	2.81	MET106	ILE554
	GLU124	THR564	2.84	MET106	PHE558
	MET141	ASN562	2.92	MET106	THR564
				ASN108	VAL550
				LEU109	VAL550
				LEU109	ILE554
				LEU109	SER551
				LEU109	GLY553
				GLU111	ILE554
				GLU111	GLN555
				LEU113	PHE558
				MET121	GLY565
				MET121	PHE558
				MET121	THR564
				GLU124	THR564
				VAL133	GLY565
				PHE138	GLY565
				PHE138	PRO563
				MET141	GLY561
				MET141	ASN562
				MET141	THR564
				MET142	PRO563
				ALA144	THR564

Comparative MD Simulation Analysis for CALM in Complex with P68(PepIQ)

To analyze the conformational changes and stability of CALM^{-WT} and CALM$^{-ASN553ILE}$ in complex with P68 (Pep-IQ), their secondary structures were evaluated by plotting RMSD and RMSF values.

RMSD, RMSF Analysis of Unbound and Bound CALM^{-WT} and CALM$^{-ASN53ILE}$ with P68(Pep-IQ)

The conformational changes and the stability of secondary structure elements were evaluated by plotting the RMSD of simulated complexes that were obtained throughout the MD trajectory. Our analysis indicated that RMSD profile of the docked complexes exhibited quite stable interacting pattern. RMSD analysis of apo (CALM^{-WT} and CALM$^{-ASN53ILE}$) and bound (CALM^{-WT} and CALM$^{-ASN53ILE}$) over the time scale of 150 ns. All the complexes got the stability between 0.4-1 nm. The apo-CALM^{-WT}, CALM^{-WT}-PepIQ, and apo-CALM$^{-ASN53ILE}$ got stability at 30 ns, while CALM$^{-ASN53ILE}$-PepIQ got stability at 60 ns. Whereas, RMSF plots indicated the residual flexibility upon binding of normal CALM^{-WT} with P68 (Pep-IQ) and mutant CALM$^{-ASN53ILE}$ with P68(Pep-IQ) throughout the simulation time. The high residual fluctuations of apo-CALM^{-WT} ASP95 (2.0-5.5Å), CALM^{-WT}-Pep-IQ LEU4(2.0-6.0 Å), PHE65 (2.0-4.0 Å), apo-CALM$^{-ASN53ILE}$ VAL139 (2.0-4.0Å), CALM$^{-ASN53ILE}$-Pep-IQ GLY23 (3.0-6.0 Å), GLY40 (2.0-6.0Å), ASP58 (3.0-7.0Å), GLY113(2.0-6.0Å), ILE130 (4.0-6.0Å). The detailed illustration is listed in Figure 11.

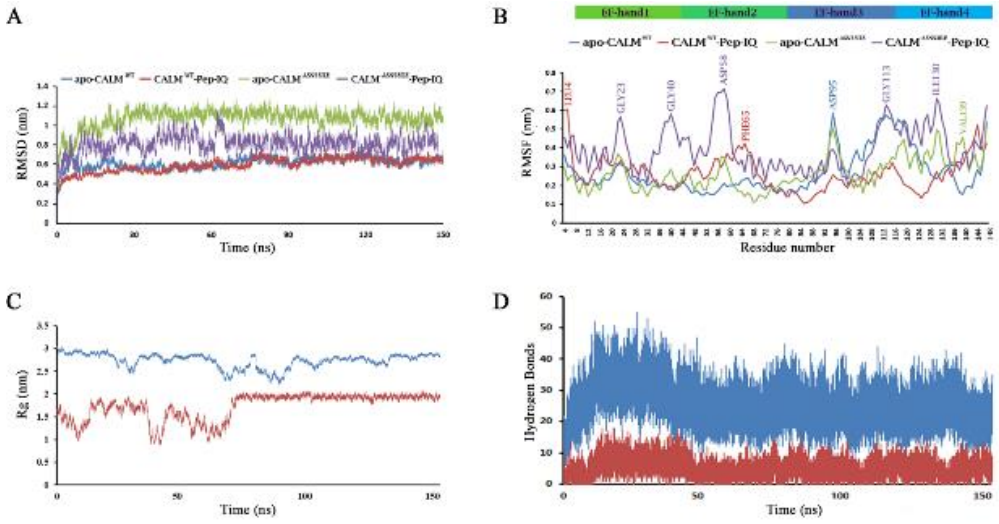

Figure 11. Time-dependent analysis to investigate stability and residual fluctuations of apo (CALM^{-WT} and CALM$^{-ASN53ILE}$) and bound (CALM^{-WT} and CALM$^{-ASN53ILE}$). (A) RMSD plot over a function of time. (B) Comparative RMSF plots for Apo-CALM^{-WT} (blue), CALM^{-WT}-PepIQ (red), apo- CALM$^{-ASN53ILE}$ (green), and CALM$^{-ASN53ILE}$-PepIQ (purple) with the corresponding secondary structures. (C) Radius of gyration plot of CALM^{-WT} and CALM$^{-ASN53ILE}$ with Pep-IQ over the 150 ns simulation time. (D) Comparison of hydrogen bonding. (For interpretation of the references to color in this figure legend, the reader is referred to the Web version of this article

Hydrogen Bond, Structural Analysis of Bound and Un-bound CALM^{-WT} and CALM$^{-ASN53ILE}$ with P68(Pep-IQ)

The Hydrogen bonding profile of CALM^{-WT} and CALM$^{-ASN53ILE}$ with p68 peptide was significantly different due to peptide binding at different regions in CALM^{-WT} and CALM$^{-ASN53ILE}$ bounded with N-terminal and C-terminal, respectively Figure 12. There was also introduction of β1 and β2 between α1-α2 and α3-α4 along with movement of C-terminal approximately to 180^0 in the apo-CALM-ASN53ILE shown in Figure 13.

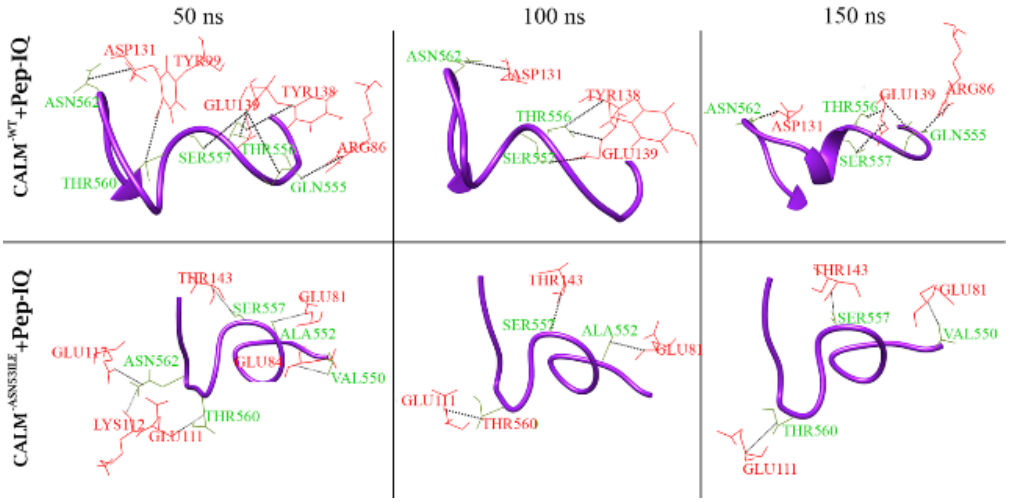

Figure 12. Hydrogen bond profiling of CALM^{-WT} and CALM$^{-ASN53ILE}$ with P68(Pep-IQ) (A & B) Hydrogen bonding pattern between CALM^{-WT} and CALM$^{-ASN53ILE}$ with Pep-IQ of p68. CALM^{-WT} and CALM$^{-ASN53ILE}$ residues are shown and labeled in red color while P68(Pep-IQ) residues are shown and labeled in green color. The Dotted lines in black color represent hydrogen bonds

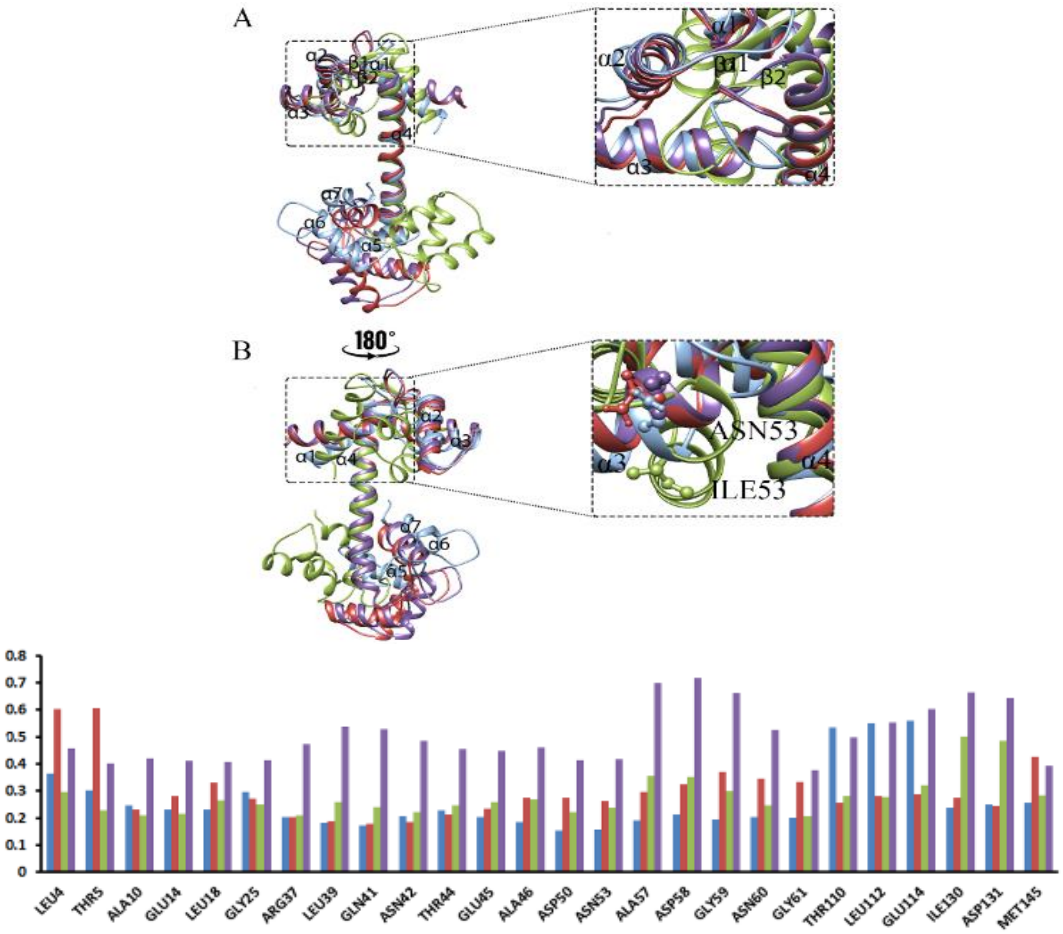

Figure 13. Super imposition to assess conformational changes in apo (CALM^{-WT}, CALM$^{-ASN53ILE}$) and bound (CALM^{-WT} and CALM$^{-ASN53ILE}$). The Conformational changes are due to induction of mutation and secondary structural changes in CALM. **(A & B)** Front and back side of CALM. **(C)** Induction of β1 and β2 in apo-CALM$^{-ASN53ILE}$ **(D)** Zoom-in view of α3 with ASN53 (wild type) and ILE53 (mutated) amino acid. Apo-CALM^{-WT} (blue), CALM^{-WT}-PepIQ (red), apo- CALM$^{-ASN53ILE}$ (green), CALM$^{-ASN53ILE}$- PepIQ (purple). Wild type and mutated amino acids are shown in corresponding and labeled in black color

Conclusions

The impact of mutation in CALM-WT and P68(Pep-IQ) binding was observed by monitoring the structural changes. Through alternative deletion of 4 Ca+2 ions (one by one) of CALM, we did not observe any change in the binding of CALM-WT and CALM-ASN53ILE with P68(Pep-IQ). In contrast, the binding pattern of P68(Pep-IQ) changed drastically due to the mutation in the (CALM-ASN53ILE). Our analysis suggested that ASN53ILE substitution in CALM may alter the P68(Pep-IQ) domain's interaction paradigm, which may lead to neuropathy. The current study may constitute a valuable starting point for CPVT therapeutics by involving the CALM-P68(Pep-IQ) complex and designing novel inhibitors to cope with neuropathological disorders.

Conflicts of Interest

The author(s) declare(s) that there is no conflict of interest regarding the publication of this paper.

Acknowledgment

We are extremely thankful for the priceless support and encouragement given by individuals from the Functional Informatics Lab, National Center for Bioinformatics.

References

[1] A. R. Pérez-Riera, R. Barbosa-Barros, M. P. de Rezende Barbosa, R. Daminello-Raimundo, A. A. de Lucca Jr, and L. C. de Abreu. (2018). Catecholaminergic polymorphic ventricular tachycardia, an update. *Ann. Noninvasive Electrocardiol.*, *23*(4), e12512.

[2] D. Reid, M. Tynan, L. Braidwood, and G. Fitzgerald. (1975). Bidirectional tachycardia in a child. A study using His bundle electrography. *Heart*, *37*(3), 339-344.

[3] K. Kistamas, R. Veress, B. Horvath, T. Banyasz, P. P. Nanasi, and D. A. Eisner. (2020). Calcium handling defects and cardiac arrhythmia syndromes. *Front. Pharmacol., 11*, 72.

[4] F. Van Petegem. (2012). Ryanodine receptors: structure and function. *J. Biol. Chem*., *287*(38), 31624-31632.

[5] J. T. Lanner, D. K. Georgiou, A. D. Joshi, and S. L. Hamilton. (2010). Ryanodine receptors: structure, expression, molecular details, and function in calcium release. *Cold Spring Harb. Perspect. Biol., 2*(11), a003996.

[6] W. J. Chazin and C. N. Johnson. (2020). Calmodulin mutations associated with heart arrhythmia: a status report. *Int. J. Mol. Sci.*, *21*(4), 1418.

[7] M. Ben-Johny and D. T. Yue. (2014). Calmodulin regulation (calmodulation) of voltage-gated calcium channels. *J. Gen. Physiol., 143*(6), 679-692.

[8] K. Kontula, P. J. Laitinen, A. Lehtonen, L. Toivonen, M. Viitasalo, and H. Swan. (2005). Catecholaminergic polymorphic ventricular tachycardia: recent mechanistic insights. *Cardiovasc. Res., 67*(3), 379-387.

[9] M. Nyegaard *et al.* (2012). Mutations in calmodulin cause ventricular tachycardia and sudden cardiac death. *The American Journal of Human Genetics*, *91*(4), 703-712.

[10] T.-Y. Dai *et al*. (2014). P68 RNA helicase as a molecular target for cancer therapy. *J. Exp. Clin. Cancer Res., 33*(1), 1-8.

[11] R. Janknecht. (2010). Multi-talented DEAD-box proteins and potential tumor promoters: p68 RNA helicase (DDX5) and its paralog, p72 RNA helicase (DDX17). *American Journal of Translational Research, 2*(3), 223.

[12] H. Wang, X. Gao, J. J. Yang, and Z.-R. Liu. (2013). Interaction between p68 RNA helicase and Ca2+-calmodulin promotes cell migration and metastasis. *Nature Communications*, *4*(1), 1354.

[13] S. F. Altschul *et al.* (1997). Gapped BLAST and PSI-BLAST: A new generation of protein database search programs. *Nucleic Acids Research*, *25*(17), 3389-3402.

[14] B. Webb and A. Sali. (2017). Protein structure modeling with MODELLER. *Functional Genomics: Methods and Protocols,* 39-54.

[15] E. F. Pettersen *et al*. (2004). UCSF Chimera—A visualization system for exploratory research and analysis. *Journal of Computational Chemistry, 25*(13),1605-1612.

[16] Y. Wardi. (1988). A stochastic steepest-descent algorithm. *Journal of Optimization Theory and Applications, 59*, 307-323.

[17] Y. Dai, J. Han, G. Liu, D. Sun, H. Yin, and Y.-x. Yuan. (2000). Convergence properties of

nonlinear conjugate gradient methods. *SIAM Journal on Optimization*, *10*(2), 345-358.
[18] E. C. Meng, E. F. Pettersen, G. S. Couch, C. C. Huang, and T. E. Ferrin. (2006). Tools for integrated sequence-structure analysis with UCSF Chimera. *BMC Bioinformatics, 7*, 1-10.
[19] V. B. Chen *et al.* (2010). MolProbity: All-atom structure validation for macromolecular crystallography. *Acta Crystallogr. Sect. D. Biol. Crystallogr., 66*(1), 12-21.
[20] C. Zhang, G. Vasmatzis, J. L. Cornette, and C. DeLisi. (1997). Determination of atomic desolvation energies from the structures of crystallized proteins. *Journal of Molecular Biology*, *267*(3), 707-726.
[21] D. Kozakov, R. Brenke, S. R. Comeau, and S. Vajda. (2006). PIPER: An FFT-based protein docking program with pairwise potentials. *Proteins: Structure, Function, and Bioinformatics*, *65*(2), 392-406.
[22] D. Kozakov *et al.* (2013). How good is automated protein docking? *Proteins: Structure, Function, and Bioinformatics*, *81*(12), 2159-2166.
[23] M. J. Abraham *et al*. (2015). GROMACS: High performance molecular simulations through multi-level parallelism from laptops to supercomputers. *SoftwareX, 1*, 19-25.
[24] I. McDonald. (1972). NpT-ensemble Monte Carlo calculations for binary liquid mixtures. *Molecular Physics*, *23*(1), 41-58.